Magnetism and interface properties of epitaxial Fe films on high-mobility GaAs/Al$_{0.35}$Ga$_{0.65}$As(001) two-dimensional electron gas heterostructures

B. Roldan Cuenya,[a] M. Doi,[b] and W. Keune[c]
Angewandte Physik, Gerhard-Mercator-Universität, D-47048 Duisburg, Germany

S. Hoch, D. Reuter, and A. Wieck
Angewandte Festkörperphysik, Ruhr-Universität Bochum, D-44780 Bochum, Germany

T. Schmitte and H. Zabel
Experimentalphysik/Festkörperphysik, Ruhr-Universität Bochum, D-44780 Bochum, Germany

An optimized heterostructure design and an optimized surface sputter-cleaning procedure allow the growth of high-quality epitaxial Fe(001) thin films at $T_s < \sim 50\,°C$ on selectively doped GaAs/Al$_{0.35}$Ga$_{0.65}$As heterostructures, while retaining the high quality transport property of the two-dimensional electron gas. Magneto-optic Kerr effect measurements and model calculations indicate a dominant uniaxial in-plane anisotropy (easy axis along [110], hard axis along [1−10]) and small coercivity ($\sim$15 Oe). Interface sensitive ^{57}Fe Mössbauer measurements prove the absence of both magnetic "dead layers" and "half-magnetization" phases (compared to pure Fe), and provide evidence for intermixing within a few monolayers, retaining, however, a metallic Fe state and high Fe magnetic moments at the interface. © 2003 American Institute of Physics. [DOI: 10.1063/1.1542934]

Ferromagnetic metal (FM)/semiconductor (SC) heterostructures are of considerable current interest due to their potential use in future magnetoelectronics devices.[1] Examples are the suggested (but not yet realized) spin devices that are based on injection of spin polarized electrons from the FM layer into the two-dimensional electron gas (2DEG) SC heterostructure.[2] Fe on GaAs is one of the model systems for the epitaxial growth of a FM on a SC.[3–9] The absence of a magnetic dead layer at the interface between Fe grown by molecular beam epitaxy (MBE) at a substrate temperature $T_s < \sim 50\,°C$ and the Ga-terminated GaAs(001) (bulk) crystal surface has been directly measured by interface-sensitive ^{57}Fe conversion-electron Mössbauer spectroscopy (CEMS),[10] in agreement with previous magnetometric results.[7,8] Further, the recently observed injection of spin polarized electrons from epitaxial Fe(001) films into GaAs(001)-based light emitting diodes[11,12] implies the presence of FM high-moment interface layers in these systems.

An issue of paramount importance is to ensure a proper function of the 2DEG after growth and lithographic treatment of the Fe film. One of the standard procedures of cleaning the surface of commercial GaAs(001) wafers in ultrahigh vacuum prior to Fe deposition is intensive sputtering at elevated temperatures ($\sim$500–600 °C) with low-energy Ar ions[7–10,13] and subsequent annealing. For standard GaAs/Al$_x$Ga$_{1-x}$As heterostructures (denoted type 1) with the typical layer sequence GaAs:Si (5 nm)/Al$_{0.35}$Ga$_{0.65}$As:Si (60 nm)/Al$_{0.35}$Ga$_{0.65}$As(60 nm)/GaAs (600 nm)/ AlAs (5.4 nm)/[GaAs (5 nm)/GaAs (50 nm)]$_{10}$/GaAs (001) wafer,

this surface cleaning process usually destroys the 2DEG. We attribute the damage to the 2DEG to the intensive Ar sputtering at rather high temperatures. We also suspect that possibly the whole GaAs:Si cap layer (only 5 nm thick) is removed during this surface cleaning process resulting in an exposed Al$_{0.35}$Ga$_{0.65}$As layer which reacts with oxygen from the air.

Besides changing the surface-cleaning process parameters (see later), we prepared heterostructures (type 2) with a considerably thicker (30 nm) GaAs cap layer to reduce the danger of exposing the Al containing layer. Only the topmost 5 nm of the GaAs cap layer was Si doped to avoid parallel conduction in this layer. Otherwise the composition of the type-2 heterostructures was the same as that of type 1. The type-2 heterostructures (substrates) were removed from the semiconductor MBE system and exposed to air. They were cleaned by 2-propanol prior to being loaded into a MBE system for metal films (base pressure 9×10^{-11} mbar). A gentle cleaning procedure was used for type-2 substrates: Ar sputtering for 15 min at only 500 eV (current density 1 μA/cm^2) at perpendicular incidence was employed to reduce the sputter yield and the crystal damage. Also the temperature during sputtering was lowered to 450 °C to minimize the As loss. After sputtering extensive annealing at 500 °C for 12 h was performed. After this treatment no surface impurities were detected by Auger electron spectroscopy, and the observed reflection high-energy electron diffraction (RHEED) pattern [Fig. 1(a)] showed streaky fundamental reflections of the clean GaAs(001) surface. However, only very faint indications of half-integer reflections from the pseudo-(4×6) surface reconstructions[7,10] of the Ga-terminated surface are visible in Fig. 1(a), indicating that surface ordering is not yet complete.

Fe film growth on this substrate surface was performed

[a]Present address: Department of Chemical Engineering, University of California at Santa Barbara, Santa Barbara, CA 93106.
[b]Present address: Department of Materials Science and Engineering, Nagoya University, Nagoya 464-8603, Japan.
[c]Electronic mail: keune@uni-duisburg.de
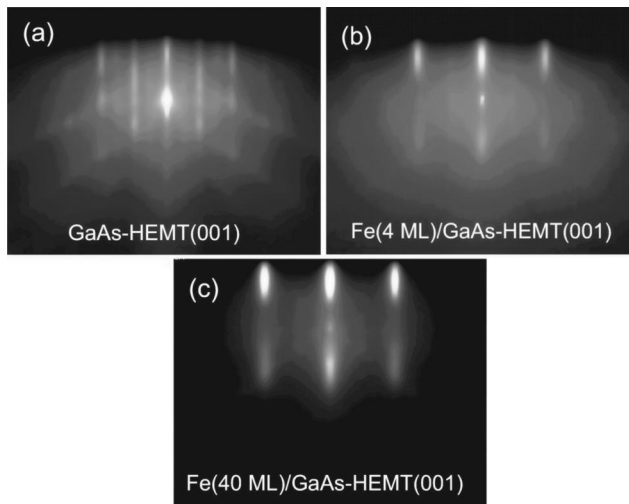
FIG. 1. RHEED patterns along the [110] azimuthal direction of the clean GaAs/Al$_{0.35}$Ga$_{0.65}$As(001)-high electron mobility transistor (HEMT) substrate surface (a), covered by 4 ML Fe(001) (b), and 40 ML Fe(001) (c). (Electron energy: 9 keV).

by first depositing 7.2 Å [5 monolayers (ML)] of 95% enriched ^{57}Fe isotope, followed by 70 Å of natural Fe (with 2% ^{57}Fe abundance), at a deposition pressure $<2\times10^{-9}$ mbar and a deposition rate of 0.03 Å/s or 1.26 ML/min. The Fe film was coated by 40 Å of Sn for protection. The growth temperature was nominally at RT; however, T_s actually rose to ~40–50 °C during deposition, as measured by a thermocouple at the sample holder surface. After deposition of 4 ML Fe and above, spotty fundamental reflections in the RHEED patterns [Figs. 1(b) and 1(c)] develop which indicate both, epitaxial growth of bcc–Fe(001) (with the in-plane [100] axes of Fe(001) and GaAs(001) aligned)[3,10,14] and rather three-dimensional (island) growth of Fe.[10,14]

Longitudinal magneto-optic Kerr effect (MOKE) hysteresis curves were measured *ex situ* at RT with different in-plane rotational angles ϕ_H between the in-plane applied field H and the in-plane crystallographic axes of the substrate (Fig. 2, insets). A small coercive field, H_c, of 15 ± 5 Oe is measured for all directions ϕ_H. The ϕ_H dependence of the magnetic remanence (Fig. 2, full squares) indicates the superposition of an in-plane twofold (uniaxial) magnetic an-

isotropy and an in-plane fourfold anisotropy. The uniaxial anisotropy has hard axes at $\phi_H=90°$ and 270°, i.e., along the $[1-10]$ direction of the substrate, and easy axes along [110], in agreement with earlier reports[9,10] about Fe films on bulk GaAs(001), but at variance with the $[1-10]$ easy-axis direction reported in Ref. 8. The fourfold hard axes are observed at $\phi_H=0°$, 90°, 180°, and 270°, i.e., along $[-1-10]$, $[1-10]$, etc., and easy direction along $[0-10]$, [100], etc., as expected for bulk bcc Fe. The origin of the fourfold anisotropy is the crystalline cubic anisotropy of bcc Fe, while the uniaxial anisotropy is due to interface anisotropy.[9]

In order to describe the measured remanence (Fig. 2), we assume a coherent in-plane rotation of the magnetization vector. The total magnetic energy is given by the sum of the Zeeman energy, the cubic and the uniaxial anisotropy energy:

$$E(\phi,H) = -\mu_0 M_s H \cos(\phi-\phi_H) + (K_1/4)\sin^2(2\phi)$$
$$+ K_U \sin^2(\phi-\phi_U). \quad (1)$$

ϕ, ϕ_H, and ϕ_U are the angles between the coordinate axis and the magnetization vector M_s, the applied field H, and the uniaxial easy axis, respectively, all oriented in the film plane. The magnetization-versus-field curve is a trajectory on the energy surface $E(\phi,H)$ starting at the maximum applied field (with M_s and H aligned), and ϕ traveling through a local minimum on the energy surface upon decreasing H. From the values $\phi(H=0)$ on this trajectory the remanence of the hysteresis loop can be calculated. (In the actual simulation a small field value of $H=10$ Oe prior to field reversal was chosen rather than $H=0$.) The magnetization curves for different in-plane angles ϕ_H were simulated using this model. From each simulation the angle ϕ at a small field ($H=10$ Oe) is recorded, and the low-field magnetization, M_1, is calculated according to $M_1(10$ Oe$) = M_s \cos[\phi(10$ Oe$)-\phi_H]$. The resulting function $M_1 = M_1(\phi_H)$, normalized to M_s, is compared to the experimental data. The full-drawn line in Fig. 2 is the result of the simulation, where the following magnetic parameters (as extracted from superconducting quantum interference device magnetometry and Ferromagnetic resonance (FMR) measurements on epitaxial Fe (77 Å)/GaAs (001))[15] were used: $M_s=1.67\times10^6$ A/m, $K_1=3.3\times10^4$ J/m^3, $K_U=1.8\times10^4$ J/m^3, and $\phi_U=45°$ {=angle between $[1-10]$ (hard axis of K_U) and [100] (easy axis of K_1)}. Our experimental and simulated data are in good agreement (Fig. 2). Moreover, the FMR parameters K_1 and K_U used here are in fair agreement with the corresponding MOKE parameters (denoted K_1^{eff} and K_U^{eff}) of high-quality epitaxial Fe(001) on bulk GaAs(001) obtained from Fig. 3 in Ref. 9 for $t_{Fe}=53.7$ ML (or 77 Å Fe): $K_1^{eff}=3.7\times10^4$ J/m^3 and $K_U^{eff}=1.6\times10^4$ J/m^3.

The predominant signal (83%) of the ^{57}Fe CEM spectrum should originate from the buried ^{57}Fe interface layer (7.2 Å), and only 17% from the natural Fe overlayer (70 Å). Thus, the Fe/GaAs interface signal is selectively enhanced in this sample. The observed spectrum (Fig. 3) was least-squares fitted in terms of two Zeeman-split subspectra. The first Zeeman sextet (which experimentally contributes to 25% of the total spectral area) shows sharp Lorentzian lines, a magnetic hyperfine (hf) field (B_{hf}) of (33.10 ± 0.04) T, and an isomer shift (chemical shift) δ of (-0.002 ± 0.004) mm/s (relative to bulk bcc Fe at RT), in accordance with the spec-

FIG. 2. MOKE results for Fe (70 Å)/^{57}Fe (7.2 Å)/GaAs/Al$_{0.35}$Ga$_{0.65}$As(001)-HEMT. The squares denote the measured values of the Kerr rotation angle at remanence, θ_K^{rem} normalized to θ_K^{sat} at saturation. The full-drawn line is the result of a model calculation. The insets show some typical Kerr hysteresis loops for $\phi_H=90°$, 180°, and 333°, as indicated.
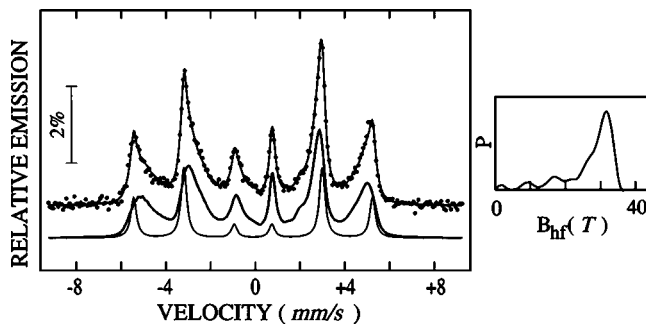
FIG. 3. Room-temperature Mössbauer (CEM) spectra and corresponding hyperfine-field distribution $P(B_{hf})$ of Fe (70 Å)/^{57}Fe (7.2 Å)/ GaAs/Al$_{0.35}$Ga$_{0.65}$As(001)-HEMT.

FIG. 4. Longitudinal resistance, R_{xx}, at 1.3 K as a function of the applied field, $B = \mu_0 H$, of a GaAs/Al$_{0.35}$Ga$_{0.65}$As-HEMT heterostructure after removal of the deposited Fe film.

tral parameters of pure bulk bcc Fe. The second Zeeman sextet (75% of the total spectral area) exhibits very broad asymmetric lines, and hence, was fitted by a distribution of hf fields, $P(B_{hf})$, including a linear correlation of B_{hf} and δ. A small positive average isomer shift $\langle\delta\rangle$ of +0.19 mm/s (corresponding to a small decrease of the s-electron density at the ^{57}Fe nucleus relative to pure bcc Fe) was obtained for the second sextet indicating a metallic Fe state. This value and the hf field distribution $P(B_{hf})$ characterize the intermixed Fe/GaAs(001) interface region. $P(B_{hf})$ shows a main peak at $B_{hf}^{peak} = (32.0 \pm 0.5)$ T and a tail that extends to lower field values due to the effect of dilute neighboring As or (more likely) Ga impurity atoms in the bcc Fe matrix[16,17] near the interface. From the very small spectral area extending to the $P(B_{hf})$ region around zero hf field it is estimated that the nonmagnetic contribution at the interface of the 7.2-Å-thick ^{57}Fe probe layer effectively amounts to only ~2% of the total area below $P(B_{hf})$. Since this corresponds to only ~0.14 Å or ~0.1 ML of ^{57}Fe, a magnetic dead layer at this interface can be ruled out. Moreover, the peak hf field $B_{hf}^{peak} = 32.0$ T and the measured average hf field $\langle B_{hf}\rangle = (27.0 \pm 0.2)$ T have rather high values. Using the usual conversion factor of ~15 T/μ_B[18] for bcc Fe alloys, we deduce corresponding Fe atomic moments of ~2.1 and ~1.8 μ_B, respectively. This provides evidence for the presence of high Fe atomic moments at our Fe/GaAs(001) interface, similar to those observed in ferromagnetic dilute bcc Fe-base FeGa and FeAs alloys,[17] and the absence of half-magnetization phases.[6] Our finding explains the high spin injection efficiency recently observed in Fe/GaAs(001)-based light emitting diodes.[12]

The most interesting result of our investigation is exhibited in Fig. 4. Here, the longitudinal magnetoresistance R_{xx} at 1.3 K as a function of the magnetic field $B = \mu_0 H$ is shown for an optimized GaAs/Al$_{0.35}$Ga$_{0.65}$As(001) heterostructure (type 2) that had been subjected to the surface cleaning procedure described earlier and had been covered by an epitaxial Fe(70 Å)/^{57}Fe(7.2 Å) film. Before recording the R_{xx} data, the Fe film was removed by HCl etching in order to avoid an electrical shunt. One clearly observes the fingerprint of a 2DEG without parallel conduction, i.e., the Shubnikov–deHaas oscillations at low fields, the pronounced minima at integer filling factors, and the drop to zero for R_{xx}
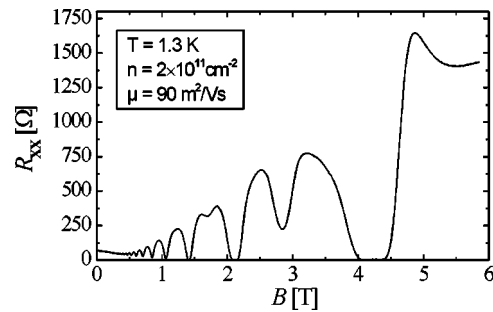
at low filling factors. The electron density without illumination was 2.05×10^{11} cm^{-2}, and a mobility of 90 m^2/V s was observed. This agrees within 15% with the values determined for a reference heterostructure (type 2) that was not subjected to the surface cleaning procedure and had no Fe film deposited. This implies that the optimized heterostructure design and surface cleaning procedure used here allow a sufficient surface preparation for the growth of magnetic-dead-layer free epitaxial Fe films, while maintaining the integrity of the high-quality 2DEG.

[1] G. A. Prinz, Science **250**, 1092 (1990); Phys. Today **48**, 58 (1995).
[2] S. Datta and B. Das, Appl. Phys. Lett. **56**, 665 (1990).
[3] G. A. Prinz and J. J. Krebs, Appl. Phys. Lett. **39**, 397 (1981); J. J. Krebs, B. T. Jonker, and G. A. Prinz, J. Appl. Phys. **61**, 2596 (1987).
[4] C. Daboo, R. J. Hicken, E. Gu, M. Gester, S. J. Gray, D. E. P. Eley, E. Ahmad, and J. A. C. Bland, Phys. Rev. B **51**, 15964 (1995); E. Gu, J. A. C. Bland, C. Daboo, M. Gester, L. M. Brown, R. Ploessl, and J. N. Chapman, *ibid.* **51**, 3596 (1995); M. Gester, C. Daboo, R. J. Hicken, S. J. Gray, A. Ercole, and J. A. C. Bland, J. Appl. Phys. **80**, 347 (1996); M. Gester, C. Daboo, S. J. Gray, and J. A. C. Bland, J. Magn. Magn. Mater. **165**, 242 (1997).
[5] E. M. Kneedler, B. T. Jonker, P. M. Thibado, R. J. Wagner, B. V. Shanabrook, and L. J. Whitman, Phys. Rev. B **56**, 8163 (1997).
[6] A. Filipe, A. Schuhl, and P. Galtier, Appl. Phys. Lett. **70**, 129 (1997); A. Filipe and A. Schuhl, J. Appl. Phys. **81**, 4359 (1997); **83**, 3077 (1998).
[7] M. Zölfl, M. Brockmann, M. Köhler, S. Kreuzer, T. Schweinböck, S. Miethaner, F. Bensch, and G. Bayreuther, J. Magn. Magn. Mater. **175**, 16 (1997).
[8] Y. B. Xu, E. T. M. Kernohan, D. J. Freeland, A. Ercole, M. Tselepi, and J. A. C. Bland, Phys. Rev. B **58**, 890 (1998).
[9] M. Brockmann, M. Zölfl, S. Miethaner, and G. Bayreuther, J. Magn. Magn. Mater. **198–199**, 384 (1999).
[10] M. Doi, B. Roldan Cuenya, W. Keune, T. Schmitte, A. Nefedov, H. Zabel, D. Spoddig, R. Meckenstock, and J. Pelzl, J. Magn. Magn. Mater. **240**, 407 (2002).
[11] H. J. Zhu, M. Ramsteiner, H. Kostial, M. Wassermeier, H.-P. Schönherr, and K. H. Ploog, Phys. Rev. Lett. **87**, 016601 (2001).
[12] A. T. Hanbicki, B. T. Jonker, G. Itskos, G. Kioseoglou, and A. Petrou, Appl. Phys. Lett. **80**, 1240 (2002).
[13] J. W. Freeland, I. Coulthard, W. J. Antel, Jr., and A. P. J. Stampfl, Phys. Rev. B **63**, 193301 (2001).
[14] C. Lallaizon, B. Lepine, S. Ababou, A. Schussler, A. Quemerais, A. Guivarc'h, G. Jezequel, S. Deputier, and R. Guerin, Appl. Surf. Sci. **123/124**, 319 (1998).
[15] R. Meckenstock, D. Spoddig, K. Himmelbauer, H. Krenn, M. Doi, W. Keune, Z. Frait, and J. Pelzl, J. Magn. Magn. Mater. **240**, 410 (2002).
[16] L. R. Newkirk and C. C. Tsui, Phys. Rev. B **4**, 4046 (1971).
[17] I. Vincze and A. T. Aldred, Phys. Rev. B **9**, 3845 (1974).
[18] P. C. M. Gubbens, J. H. F. van Apeldoorn, A. M. van der Kraan, and K. H. J. Buschow, J. Phys. F: Met. Phys. **4**, 921 (1974).